

## II.E.4 Solar-Thermal ALD Ferrite-Based Water Splitting Cycle

Alan W. Weimer (Primary Contact), Darwin Arifin,  
Xinhua Liang, Victoria Aston and Paul Lichty  
University of Colorado  
Campus Box 596  
Boulder, CO 80309-0596  
Phone: (303) 492-3759  
Email: alan.weimer@colorado.edu

### DOE Manager

HQ: Sara Dillich  
Phone: (202) 586-7925  
Email: Sara.Dillich@ee.doe.gov

Contract Number: DE-FC36-05GO15044

Project Start Date: March 31, 2005

Project End Date: Project continuation and direction  
determined annually by DOE

### Fiscal Year (FY) 2012 Objectives

- Demonstrate the “hercynite cycle” feasibility for carrying out redox.
- Initiate design, synthesis and testing of a nanostructured active material for fast kinetics and transport.
- Demonstrate the “hercynite cycle” on-sun.

### Technical Barriers

This project addresses the following technical barriers from the Production section, page 3.1-26 of the Fuel Cell Technologies Program Multi-Year Research, Development and Demonstration Plan:

- (U) High-Temperature Thermochemical Technology
- (V) High-temperature Robust Materials
- (W) Concentrated Solar Energy Capital Cost
- (X) Coupling Concentrated Solar Energy and Thermochemical Cycles

### Technical Targets

The technical targets for solar-driven thermochemical conversion are summarized in Table 1. The projected thermal efficiency for the developed process is 55.5% lower heating value (LHV), thus exceeding the >35% requirement for the 2017 case. For a solar to receiver annual average efficiency of 40.2%, the overall solar to H<sub>2</sub> efficiency is estimated at 22.3% (LHV). Current results indicate that it is possible to achieve

**TABLE 1.** Technical Targets for Solar-driven High-Temperature Thermochemical Hydrogen Production

Characteristics	Units	2012 Target	2017 Target
Plant Gate H <sub>2</sub> Cost	\$/gge H <sub>2</sub>	\$6	\$3
Installed Heliostat Capital Cost	\$/m <sup>2</sup>	\$140	\$80
Process Energy Efficiency (thermal, LHV)	%	30	>35

gge – gasoline gallon equivalent

reduction times of <30 seconds and oxidation times with oxygen of <30 seconds. Oxidation with steam requires longer times, but it has been found that increased steam partial pressure substantially increases the rate of reaction. Methods to decrease redox cycle time are a focus of current research.

### FY 2012 Accomplishments

- Demonstrated redox cycles with oxygen oxidation at less than 2 minutes.
- “Hercynite cycle” reaction mechanism through stable aluminate compounds verified by Raman spectroscopy.
- Designed active material nanostructures fabricated by atomic layer deposition demonstrated stable activity after the first cycle up to 25 cycles.



### Introduction

Two-step solar thermochemical processes based on non-volatile metal oxide cycles have the potential to operate at high thermal efficiencies, are chemically simple, and require less land and water to operate than competing biomass, artificial photosynthesis and photovoltaic-driven electrolysis. Traditionally, two types of non-volatile metal oxide redox chemistries are utilized in solar thermochemical CO<sub>2</sub> splitting. The first is based on non-stoichiometric oxides of which ceria is a representative example. Such redox materials are thermally reduced without undergoing phase change, as the lattice is able to accommodate the strain induced by oxygen vacancy formation. These materials are thermally quite stable, although the extent of reduction, and hence cycle capacity, is small compared to other reducible oxides.

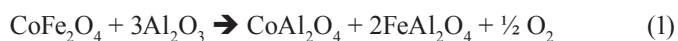
The second prototypical chemistry utilizes materials of the spinel structure that form solid solutions upon reduction. The most common are ferrites where Fe<sup>3+</sup> in M<sub>x</sub>Fe<sub>3-x</sub>O<sub>4</sub> is partially reduced to Fe<sup>2+</sup>; here M can be any number of transition metals that form spinel type oxides with iron though Co, Zn, and Ni are the most studied.

In these redox cycles, the ferrite spinel is heated until it decomposes into a mixture of metal oxide solid solutions that are thermodynamically stable at temperatures above which the spinel decomposes. Thus, thermal reduction yields a solid solution of oxides with mixed valence ( $M^{2+}$ ,  $Fe^{2+}$ , and  $Fe^{3+}$ ). While these materials theoretically exhibit greater redox potential than non-stoichiometric oxides, in practice deactivation induced by irreversible processes such as sintering or the formation of liquid phases and metal vaporization lead to loss of active oxide.

In this work, we examine a novel chemistry for a two-step, non-volatile metal oxide  $H_2O$  splitting cycle that shuttles iron oxidation states ( $Fe^{2+/3+}$ ) between  $CoFe_2O_4$  and  $FeAl_2O_4$  spinel compounds within a nano-engineered material. This chemistry is dramatically different than current metal oxide cycles that exploit oxygen non-stoichiometry in ceria or solid solution behavior in ferrites. The engineered material was prepared using atomic layer deposition (ALD) and maintained structural integrity over 6 heating cycles under conditions that mimic a concentrated solar power application, namely an oxidation temperature of  $1,000^\circ C$ , reduction at  $1,460^\circ C$ , and a heating rate of  $16^\circ C/s$  from low to high temperature. Oxygen uptake and release behavior was similar to that of ceria. Raman spectroscopy was used to verify cycle chemistry. These properties provide for a technical foundation to achieve the DOE technical targets and enable the hydrogen economy.

## Approach

So called the “hercynite cycle”, reduction chemistry occurs via a reaction between decomposition products of the  $CoFe_2O_4$  and  $Al_2O_3$ , forming the corresponding stable aluminates  $CoAl_2O_4$  and  $FeAl_2O_4$  according to the following oxygen evolution reaction:



During subsequent oxidation by  $H_2O$ , the cobalt ferrite spinel and alumina reform and  $H_2$  is produced:



The oxygen evolution reaction Eq. (1) occurs to a greater extent at a temperature  $150^\circ C$  lower than a similarly prepared  $CoFe_2O_4$ -coated m- $ZrO_2$  (conventional ferrite) because compound formation is thermodynamically more favourable than solid solution formation. While lowering the reduction temperature is an important consideration for solar thermochemical technologies, perhaps more intriguing is the idea of binding the reduced iron in a compound that is more stable than solid solution.

Inspired by these initial observations, we deposited a nanometer thick film of  $CoFe_2O_4$  on a porous thin-walled (15 nm) skeletal  $Al_2O_3$  support to study the  $CO_2$  splitting

capability of this material for use in a concentrated solar power application. The reactive structure is depicted schematically in Figure 1 along with optical images of sample material photographed in the oxidized and reduced states, and an field emission scanning electron microscope (FESEM) image of the alumina support before thermal cycling. The cartoon in Figure 1 implies that the  $CoFe_2O_4$  film is located on the exterior surface of the support shell, but the ALD process ensures that the ferrite film covers all gas-accessible surfaces on and within the porous material. As a result, the cobalt ferrite mass loading is relatively high (20%) and the reactive structure maintains a high effective surface area and low bulk density prior to high-temperature thermal cycling.

The main benefit of this reactive structure that sets it apart from prior work is that we can better engineer the spinel-alumina interface. Ideally we would like to irradiate only redox active material, any excess  $Al_2O_3$  would reduce process efficiency by heating of inert carrier. Deposition of  $CoFe_2O_4$  on either high surface area  $Al_2O_3$  powders or monoliths would be undesirable because too much inert material would end up in the structure. Perhaps more important than wasting heat, a large excess of alumina would lead to diffusion of Co and Fe deeply into the bulk and undoubtedly have a detrimental impact on the redox kinetics. The porous  $Al_2O_3$  skeletal support with 15-nm wall thickness addresses both of these concerns.

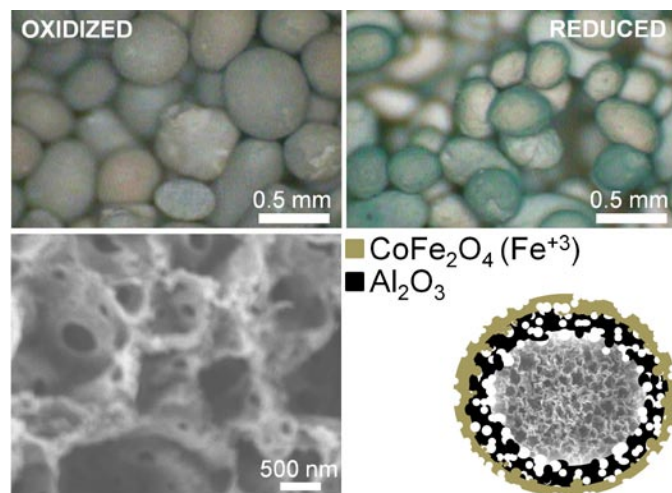


**FIGURE 1.** Optical image showing 0.5-mm diameter spheroids of porous  $Al_2O_3$  shells coated in nanometer thick  $CoFe_2O_4$ . Color changes from brown to green when hercynite forms upon thermal reduction (top). FESEM image of the porous  $Al_2O_3$  structure prepared by ALD (bottom left). Schematic illustrating the conceptual layout of the nano-engineered reactive structure, not drawn to scale, and the spinel compound that forms upon calcination (bottom right). A representative FESEM image of the skeletal structure is incorporated into the schematic. The coverage of  $CoFe_2O_4$  on the alumina scaffold is not limited to the outer surface; it coats all gas-accessible surfaces on and within the porous structure (see text).

## Results

An important measure of a material's suitability for a thermochemical water splitting cycle is the extent to which oxygen exchange occurs upon heating and cooling. This activity was assessed by exposing the nano-engineered material to a gas flow containing 2,000 ppm  $O_2$  in helium and rapidly heating and cooling the material while monitoring the  $O_2$  uptake and release behaviour. The results of this experiment are presented in Figure 2. Starting at  $t = 0$  s, a constant background of  $O_2$  is measured by the mass spectrometer. At several time intervals spaced roughly 350 s apart, a laser irradiates the sample raising the temperature from 1,000°C to 1,460°C in 30 s. After a 100 s dwell at 1,460°C, the laser power is turned off and the sample is allowed to cool through conductive, convective, and radiative processes. Testing was carried out for a total of 25 cycles.

According to the data in Figure 2, during the initial part of the heating interval the  $O_2$  signal increases to a peak that is 47% above background, then quickly falls back to baseline before the 100 s dwell time at high temperature expires.  $O_2$  evolution in a gaseous environment where the oxygen activity is relatively high (0.001 atm) indicates favorable thermodynamics for reduction at conditions relevant to solar-driven thermochemistry. Of equal importance is the observation that the material reabsorbs oxygen on cooling, which is evidenced by the  $O_2$  signal dropping below the 2,000 ppm background level for a short period of time after

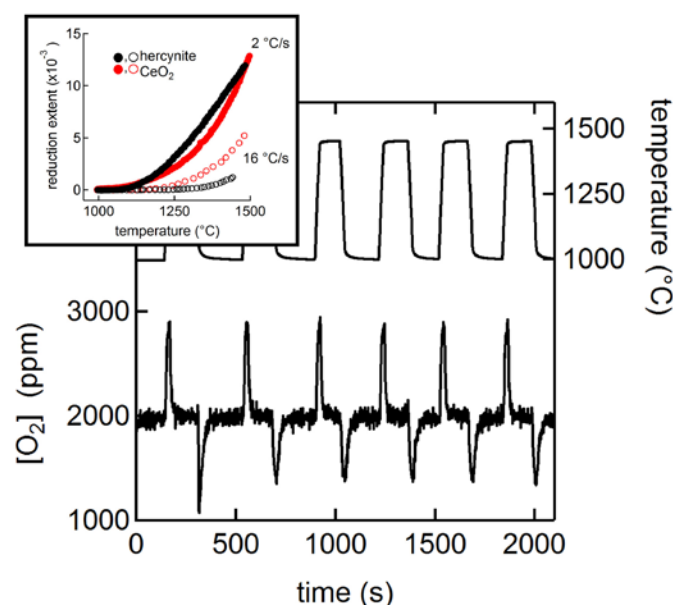


**FIGURE 2.** Oxygen uptake and release behaviour as a function of time and temperature measured in the presence of a constant 2,000 ppm  $O_2$  background partial pressure indicates thermodynamics for hercynite reduction are favorable for solar-driven thermochemical cycles (see text). The reduction extent as a function of temperature for ceria and hercynite at two different heating rates is shown in the inset.

laser irradiation. To a first approximation, the area under the desorption peak is equal to that of the absorption peak ( $\sim 100$   $\mu\text{moles } O_2/\text{g}$  of material). Furthermore, the  $O_2$  redox behavior is reproducible over 6 heating cycles indicating that the material remains chemically active and is structurally stable (i.e., no significant irreversible loss of activity, surface area, physical dimension, or metal oxide).

Optical images of the sample taken before and after thermal redox cycling (Figure 1) show that the material maintains its semi-spherical shape, however, noticeable shrinkage occurs during repeated exposures to 1,460°C. Brunauer-Emmett-Teller analysis on similarly cycled materials confirms internal structural changes that are consistent with loss of porosity and sphere volume as the surface area is reduced from 44  $\text{m}^2/\text{g}$  (as prepared) to 1.6  $\text{m}^2/\text{g}$  (cycled). This is due to collapse of the micropores and mesopores in the alumina material resulting from grain growth at these extreme temperatures. Nonetheless, after the first cycle, the oxygen capacity did not diminish after 23 thermal reductions, amounting to 20 hours at 1,000°C and 2 hours at 1,460°C, implying that the activity of the material is not affected by loss of internal surface area and that all structural changes occurred during the first cycle. A more rigorous and detailed study investigating the effect of porosity and the thermal stability of the material is currently underway.

The graph inset to Figure 2 reveals another important feature of our engineered reactive structure. Here we plot the reduction extent as a function of temperature for two different heating rates. The reduction extent is calculated by taking the ratio of evolved oxygen, integrated as a function of time on a molar basis, to the total amount of oxygen present in the fully oxidized material. There are two pieces of information available in Figure 2; (1) by comparing a slow heating rate (2  $^{\circ}C/s$ ) to a fast heating rate (16  $^{\circ}C/s$ ) possible kinetic limitations to  $O_2$  redox become evident, and (2) the reduction extent for a given temperature provides information on cycle capacity (i.e., how much fuel can be produced per a mole of material). For comparison, reduction data are also presented for  $CeO_2$  particles (nominally 5- $\mu\text{m}$  diameter) in Figure 2.

Clearly the 2  $^{\circ}C/s$  heating rate produces more  $O_2$  at a given temperature than the 16  $^{\circ}C/s$  rate, which is likely due to a transport limitation within the reactive structure. However, the nanostructured ferrite performance compares comparably to that of  $CeO_2$  which, unlike iron oxide, is known to possess high oxygen ion conductivity and rapid exchange kinetics. Therefore it is conceivable that by reducing the thickness of the  $Al_2O_3$  skeletal structure, diffusion limitations may be further mitigated allowing greater utilization of the redox active Fe cation and faster redox kinetics.

To support our hypothesis that the reactions embodied by Eqs. 1 and 2 are correct, we analyzed the chemical

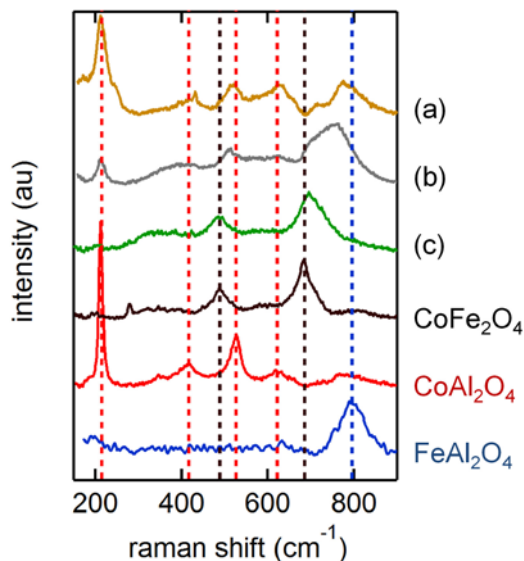


**FIGURE 3.** Surface Raman spectra recorded for ferrite and aluminate reference materials compared to unknown compositions of nano-engineered  $\text{CoFe}_2\text{O}_4$ -coated  $\text{Al}_2\text{O}_3$  material prepared by thermal reduction in helium (a), or oxidation in  $\text{CO}_2$  (b), or oxidation in  $\text{O}_2$  (c).

composition of the nanostructured materials using surface Raman spectroscopy. Several representative samples were oxidized in either  $\text{O}_2$  or  $\text{CO}_2$ , or reduced in pure helium, and then thermally quenched before ex situ examination in a Raman microscope. Presented in Figure 3 are Raman spectra for three of our endpoint compounds,  $\text{CoFe}_2\text{O}_4$ ,  $\text{CoAl}_2\text{O}_4$ , and  $\text{FeAl}_2\text{O}_4$ , along with spectra measured from samples taken at various states of oxidation (labelled a-c in the figure). Material fully oxidized in  $\text{O}_2$  (c) exhibits spectral features indicative of  $\text{CoFe}_2\text{O}_4$ , with two main excitation peaks observed at 476 and 686  $\text{cm}^{-1}$  which agrees with literature assignments for this compound. Raman spectra for material in the fully reduced state (a) show a mixture of phonon modes that can be attributed to cobalt aluminate and hercynite. Furthermore, the strong resonance features of  $\text{CoFe}_2\text{O}_4$  are not detectable in (a) indicating that the reduction reaction has gone to completion in the near surface region of the ferrite. Also of note is the relative stability of the reduced compound ( $\text{FeAl}_2\text{O}_4$ ) in air at room temperature. Samples were removed from the reactor and stored for several days before transport to the Raman microscope without special handling to avoid air exposure.

## Conclusions and Future Directions

- The “hercynite cycle” active materials follow a redox mechanism through stable aluminates which is predicted to provide for a chemically robust process.
- Our  $\text{CoFe}_2\text{O}_4$ -coated  $\text{Al}_2\text{O}_3$  material is capable of producing appreciable amounts of  $\text{H}_2$  after thermal reduction at a temperature as low as 1,360°C, with consistent oxidation behavior up to 25 thermal reductions. This observation is approximately 100°C to 150°C lower than values reported for ferrite or  $\text{CeO}_2$ -based systems, respectively.
- The nanostructured active materials can be improved to reduce diffusional resistances and work is underway to develop such materials.

## Patents Issued

1. “Metal Ferrite Spinel Energy Storage Devices and Methods for Making and Using Same,” U.S. Patent 8,187,731 (2012).

## FY 2012 Publications/Presentations

1. Arifin, D., V.J. Aston, X.H. Liang, A.H. McDaniel and A.W. Weimer, “ $\text{CoFe}_2\text{O}_4$  on Porous  $\text{Al}_2\text{O}_3$  Nanostructure for Solar Thermochemical  $\text{CO}_2$  Splitting,” *Energy and Environmental Science*; in-press, DOI:10.1039/C2EE22090C (2012).
2. Martinek, J., C. Bingham, and A.W. Weimer, “Computational Modeling and On-sun Model Validation for a Multiple Tube Solar Reactor with Specularly Reflective Cavity Walls, Part 1: Heat Transfer Model,” *Chemical Engineering Science*; **81**, 298 - 310 (2012).
3. Martinek, J., C. Bingham, and A.W. Weimer, “Computational Modeling of a Multiple Tube Solar Reactor with Specularly Reflective Cavity Walls, Part 2: Steam Gasification of Carbon,” *Chemical Engineering Science*, **81**, 285 - 297 (2012).
4. Scheffe, J.R., M.D. Allendorf, E.N. Coker, B.W. Jacobs, A.H. McDaniel and A.W. Weimer, “Hydrogen Production via Chemical Looping Redox Cycles Using Atomic Layer Deposition-Synthesized Iron Oxide and Cobalt Ferrites,” *Chemistry of Materials*, **23** (8), 2030-2038 (2011).